

## Test of the Universal Scaling Law for the Diffusion Coefficient in Liquid Metals

J. J. Hoyt<sup>1</sup>, Mark Asta,<sup>2</sup> and Babak Sadigh<sup>3</sup>

<sup>1</sup>*Sandia National Laboratories, MS 9161, P. O. Box 969, Livermore, California 94551-0969*

<sup>2</sup>*Department of Materials Science and Engineering, Northwestern University, Evanston, Illinois 60208*

<sup>3</sup>*Lawrence Livermore National Laboratory, Livermore, California 94550*

(Received 30 March 1999)

The recently proposed scaling law relating the diffusion coefficient and the excess entropy of a liquid [M. Dzугutov, *Nature (London)* **381**, 137 (1996)] is tested for several metals using molecular dynamics simulations. Interatomic potentials derived from the embedded atom method are used to study Ag, Au, Cu, Ni, Pd, Pt, Ni<sub>3</sub>Al, and AuPt and the angular dependent Stillinger-Weber form is used to investigate Si.

PACS numbers: 66.10.Cb

To understand such important material processing techniques as binary solidification and glass formation, a knowledge of the liquid state diffusion coefficient is required. Despite its fundamental importance, however, the diffusivity remains an elusive quantity. It is very difficult to measure experimentally and, unlike crystalline solids, it is not fully understood how the diffusion coefficient depends on the structure and thermodynamics of the liquid. Our current knowledge of liquid transport properties was advanced recently by Dzугutov [1] who proposed a universal scaling relationship between the excess entropy of a liquid and the diffusion coefficient. The excess entropy is the total entropy minus the ideal gas contribution.

The Dzугutov scheme is based on two main propositions. First, short range repulsive interactions govern the transfer of energy and momentum in the liquid and this interaction can be approximated by binary hard sphere collisions. Thus, the diffusion coefficient,  $D$ , is expressed in dimensionless form,  $D^*$ , via  $D^* = D\Gamma^{-1}\sigma^{-2}$ , where  $\sigma$  is the hard sphere diameter and  $\Gamma$  is the collision frequency according to the well-known Enskog theory of atomic transport [2]:

$$\Gamma = 4\sigma^2 g(\sigma)\rho \sqrt{\frac{\pi k_B T}{m}}. \quad (3)$$

Here  $g(\sigma)$  is the radial distribution function evaluated at the hard sphere diameter [in practice  $\sigma$  may be interpreted as the position of the first peak in the  $g(r)$ ],  $m$  is the mass of the diffusing species,  $\rho$  is the number density, and  $k_B T$  has the usual meaning of Boltzmann's constant times temperature.

The second idea central to the universal scaling law is that the frequency of local structural relaxations in the liquid dictates cage diffusion and is proportional to the number of accessible configurations in the system. Therefore, the normalized diffusivity  $D^*$  is proportional to  $e^S$ , where  $S$  is the excess entropy per atom expressed in units of  $k_B$ . In the original Dzугutov work the excess entropy was

approximated by the two-body approximation [3] which is denoted  $S_2$  and is given by

$$S_2 = -2\pi\rho \int_0^\infty \{g(r) \ln[g(r)] - [g(r) - 1]\} r^2 dr. \quad (2)$$

Dzугutov demonstrated the validity of the scaling law for several model liquids, including, Pb, Cu, Lennard-Jones (LJ), and hard sphere systems, but in all cases a simple pair potential was employed in the simulations. If true, the Dzугutov scaling law is a very important finding in that it links the dynamic behavior of a liquid with a static thermodynamic quantity,  $S$ , or, if the  $S_2$  approximation is valid, it provides a very elegant example of an experimentally accessible structure-property relation in a liquid. However, in order to confidently label the scaling law universal, the hypothesis must be tested with different forms of the interatomic potential, for example, multibody potentials and potentials which include angular dependent contributions. Thus it is the purpose of this Letter to test the Dzугutov idea by computing the diffusivities, radial distribution functions, and excess entropies for several liquids using atomistic computer simulations, where embedded atom potentials are used for various late transition metals and noble metals and the Stillinger-Weber (SW) scheme [4] is employed to study Si. The embedded atom method (EAM) [5,6] has been shown to yield quite accurate predictions for various structural [7,8], thermodynamic [8,9] and atom transport properties [8,10–13] of liquid metals and alloys and, as such, the scaling behavior will be tested for “real” liquids. Specifically, we have studied the pure systems Ag, Au, Cu, Ni, Pd, and Pt. For the case of Si it should be noted that the angular dependent SW scheme has been used by Yu, Wang, and Stroud [14] to study the structure and dynamics of liquid Si and Ge. This paper is confined to metal systems, Si being metallic in the liquid state [14].

Dzугutov also examined two binary mixtures. In the binary case the scaled variables for each species were found

by simply replacing the quantities  $\sigma$ ,  $\rho$ ,  $g$ , and  $m$  in Eqs. (1) and (2) with the relevant values for each individual component in the mixture. The fact that the scaling law is also obeyed for the binary construction is somewhat surprising as one would intuitively expect the partial radial distribution function  $g_{12}(r)$  and an interatomic distance between species 1 and 2 to appear in the scaling relationship. It is possible that the binary systems investigated by Dzugutov are ideal in the sense that no strong short range order exists in the liquid. Therefore, in this paper we will also extend the Dzugutov scaling law to general binary liquids and demonstrate its validity on two metallic alloys which exhibit differing degrees of chemical short range order, namely,  $\text{Ni}_3\text{Al}$  and  $\text{AuPt}$ . The Ni-Al system is characterized by a strong unlike (i.e., Ni-Al) bond, and hence the nearest neighbor shell of Ni(Al) in the liquid contains a greater than average number of Al(Ni) atoms, whereas liquid  $\text{AuPt}$  exhibits a slight preference for like bonds.

The first step in evaluating the scaling behavior is to critically test the  $S_2$  approximation of the excess entropy. Equilibrated liquid structures for various temperatures were generated using Monte Carlo (MC) simulations on periodic cells containing 2048 atoms. The equilibration was performed using  $10^5$  steps per atom, and approximately 50 configurations were employed to generate the radial distribution functions. For Ag, Au, Cu, Pd, and Pt the EAM potential due to Foiles, Baskes, and Daw [15] was utilized and, to check for possible effects due to the specific EAM parametrization, the Voter and Chen [16] potential has been used for Ni and  $\text{Ni}_3\text{Al}$ . From the equilibrated liquids, diffusion coefficients were obtained from molecular dynamics simulations using a time step of 1 fs and a total time of 50 ps. In the molecular dynamics simulations a microcanonical ensemble was used with the volume chosen from Monte Carlo simulations such that the average pressure was zero. The velocity-velocity correlation functions were obtained by averaging over all atoms in the system and over several time origins; the integral over all time of the velocity-velocity correlation functions yields the diffusion coefficient [17]. For a more detailed description of the Monte Carlo and molecular dynamics simulations, the reader is referred to Refs. [8] and [13]. A wide range of temperatures have been examined in the study. Ag, Au, Cu, Pd, and Pt were studied over the range 1500–2200 K, and for Ni and the  $\text{Ni}_3\text{Al}$  alloy a slightly larger range was investigated (1500–3000 K).

Figure 1 shows the scaled diffusion coefficient  $D^*$  [Eq. (1)] vs  $S_2$  as computed from Eq. (2), and the results are compared to the original best fit determined by Dzugutov (dashed line). Although the scaling law holds reasonably well for the pure elements, there is some scatter in the data, more so than the original Dzugutov work, and the trend with temperature appears to be slightly nonlinear [18]. It must be emphasized that the scatter exhibited in Fig. 1 does *not* necessarily invalidate the basic proposition of Dzugutov ( $\ln D^*$  is proportional to  $S$ ) but it may suggest that the  $S_2$  approximation is

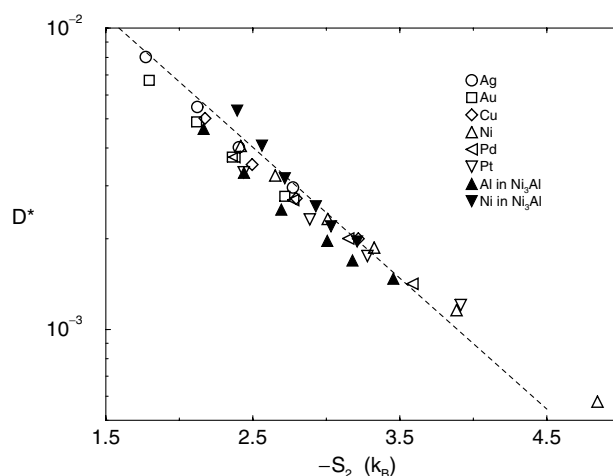


FIG. 1. The scaled diffusion coefficient vs the  $S_2$  approximation of the excess entropy for various EAM liquid metals. Entropy is expressed in units of  $k_B$ . The dashed line is the relationship found in the original work of Dzugutov.

not completely reliable when utilizing EAM potentials. Baranya and Evans [19] compared the true excess entropy, obtained via thermodynamic integration, with the  $S_2$  approximation for Lennard-Jones systems. It was found that the difference between the actual excess entropy and the approximate  $S_2$  value was nearly constant over a wide range of densities and the constant offset will merely translate into a constant shift of the data on the semilog scale of Fig. 1. In other words, it is reasonable to assume that for the simple model systems studied by Dzugutov the  $S_2$  description is a very good approximation, but for the density dependent, many-body EAM potential the approximation is less accurate. There is another important point to be gleaned from Fig. 1. The filled symbols represent the individual diffusivities of Al and Ni in the  $\text{Ni}_3\text{Al}$  binary. Since many of the points lie well off the dashed line, it is clear that the simple prescription for treating binaries proposed by Dzugutov is not accurate.

Therefore, the second step in testing the scaling law involves two procedures: (i) a more reliable determination of the excess entropy is needed and (ii) a proper scaling form for binaries must be formulated. The determination of the true excess entropy involved two separate calculations. We have computed the excess entropy for all of the elements at 1500 K by a lambda integration technique [20] using a common initial state. The common reference state is a Lennard-Jones system at reduced density  $\rho^* = 0.85$  and reduced temperature  $T^* = 0.8$ . The reduced variables correspond to a point well within the fluid region of the LJ phase diagram [21,22]. The modified and truncated LJ potential due to Broughton and Gilmer [23] was employed throughout. The lambda integration yields the Helmholtz free energy change by evaluating the statistical average  $\langle \delta E / \delta \lambda \rangle_\lambda$  ( $E$  is the potential energy), where  $\lambda$  varies from zero to unity and represents the change of the interatomic potential from the LJ state to the EAM form. Since the integration path is performed at constant temperature,

the entropy change is determined via  $\Delta S = (\Delta H - \Delta F)/k_B T$ . Since the computation of  $\Delta S$  involves the difference of two fairly large values, the Helmholtz energy change  $\Delta F$  and the enthalpy change  $\Delta H$ , the lambda integration is very sensitive to uncertainties in the statistical averaging. Therefore, the value of lambda was changed in small steps of 0.1 and at each lambda the 2048 atom cell was equilibrated for 1000 time steps and statistics were then generated for a total of 4000 time steps. The accuracy of the  $\Delta S$  computation was checked by comparing the entropy with that obtained from a Monte Carlo thermodynamic integration (see below). The values of  $\Delta S$  agree to within  $0.03k_B$ , less than the size of the symbols in Figs. 1 and 2. In addition, the uncertainty in the  $\Delta S$  computation was tested by repeating the calculations using a different LJ starting point ( $T^* = 1.25$ ,  $\rho^* = 0.75$ ). The difference in the two results was much less than the  $0.03k_B$  quoted above.

The final step in the determination of the true excess entropy is evaluating  $\Delta S$  from an initial state of 1500 K to a final state of any desired temperature. For this change we have used Monte Carlo simulations to compute the enthalpy as a function of temperature and have integrated the thermodynamic relation  $d(G/T)/dT = -H/T^2$ , where  $G$  is the Gibbs free energy. The determination of free energies and excess entropies for the binary liquid is slightly more complicated. Here thermodynamic integration is performed at constant  $T$  and  $P$  by using the relationship between composition and chemical potential differences generated from a MC simulation performed in the transmutation ensemble. Details of this procedure are described fully in Ref. [8].

As alluded to above, the second step in evaluating the Dzugutov scaling law is to formulate a scaling function for a binary mixture. The extension of the Enskog theory collision frequency [see Eq. (1)] to a binary mixture has been discussed by Jacucci and MacDonald [24]. By using their result, the relevant scaled diffusivity of species 1 in a binary liquid can be written as  $D_1^* = D_1 \chi_1^{-1}$ , where the scale factor is given by

$$\chi_1 = 4\sigma_1^4 g_{11}(\sigma_1) \rho_1 \sqrt{\frac{\pi k_B T}{m_1}} + 4\sigma_{12}^4 g_{12}(\sigma_{12}) \rho_2 \sqrt{\frac{\pi(m_1 + m_2)k_B T}{2m_1 m_2}}. \quad (3)$$

An analogous scaling variable can be defined for species 2 by simply interchanging index 1 and 2 in Eq. (3). Notice that the two particle masses now appear. In addition, the scale factor now includes the mixed species radial distribution functions  $g_{12}(r)$  and  $g_{21}(r)$  which are important for liquids exhibiting chemical short range order and it contains the effective hard sphere distance  $\sigma_{12}$  which is necessary in treating liquids with significant atomic size mismatch.

We can then define a single scaled diffusion coefficient for a binary liquid in the following way. Note that the

total excess entropy is given by  $S = c_1 S_1 + c_2 S_2$ , where  $c$  is the concentration and  $S_i$  is the partial molar entropy of species  $i$ . Furthermore, since the scaling law relates the diffusivity to  $e^S$ , it is reasonable to assume a  $D^*$  of the form

$$D^* = \left(\frac{D_1}{\chi_1}\right)^{c_1} \left(\frac{D_2}{\chi_2}\right)^{c_2}. \quad (4)$$

Figure 2 shows the main results of this investigation; it plots the log of  $D^*$  vs  $-\Delta S$  for all the simulations studied. Clearly the Dzugutov scaling law is valid for all EAM systems. With the use of a more accurate excess entropy calculation rather than the  $S_2$  form, there appears to be less scatter in the data and the linearity with temperature for a given element is obeyed very well. The scatter observed in Fig. 2 is well within the uncertainty of the lambda integration technique. The solid line in the figure represents the best fit to the data and, within the numerical uncertainty, is consistent with the scaling prediction. The least squares fit to the EAM data yielded a slope of 1.06 with an uncertainty of  $\pm 0.07$ . (The intercept differs from the Dzugutov value due to the different reference state used for the entropy calculation.) Also encouraging is the fact that the binary results (filled symbols) are consistent with the scaling law, indicating that the definitions appearing in Eqs. (3) and (4) are appropriate.

The third and final test of the Dzugutov scaling law concerns the simulation results for Si. Recall that, unlike the central force nature of the EAM potential, the SW form for Si includes angular dependent contributions to the bonding. Perhaps the most notable feature of Fig. 2 is the failure of Si to obey the scaling law. The  $D^*$  results for Si are consistently higher than the EAM data and the slope of the line is slightly lower. We believe the discrepancy shown in Fig. 2 is due to the very different liquid structure observed for Si which is a direct consequence of the strong angular bonding. The frequency term given in Eq. (1)

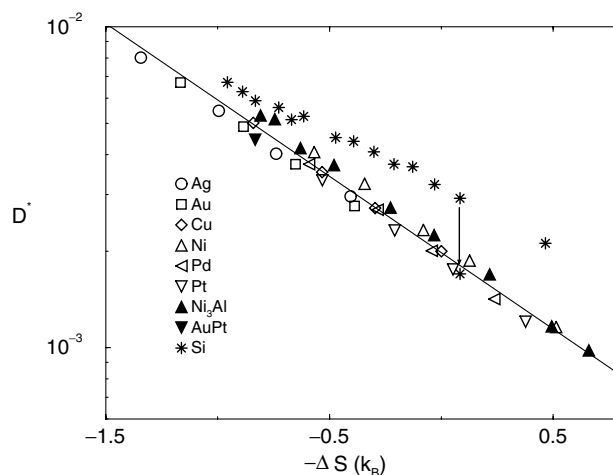


FIG. 2.  $D^*$  vs the excess entropy difference  $-\Delta S$  for the various liquid metals and alloys. The solid line is the best fit to the data. The downward pointing arrow denotes a correction to the Si data point as described in the text.

contains the average velocity of an atom in the liquid as well as the probability that a given atom will collide with its local nearest neighbor shell. In the Dzugutov formulation all details of local structure are approximated by replacing the actual  $g(r)$  in the region of the nearest neighbor distance by its value at the first peak, i.e.,  $g(\sigma)$ . In liquids characterized by central force potentials—EAM, Lennard-Jones, hard sphere, etc.—the first peak in the radial distribution is very sharp; atoms are on average surrounded by a well-defined cage and the collision frequency described by Eq. (1) is adequate. In Si the angular bonding leads to a very different liquid structure. In addition to the strong first peak in  $g(r)$  there exists a small peak on the high- $r$  side. This shoulder becomes more pronounced at lower temperatures (see, for example, Ref. [14]). Thus in Si the first neighbor shell actually consists of two closely spaced shells, and assigning a unique collision frequency as in Eq. (1) is no longer appropriate. Based on the very different structure observed for liquid Si, it is perhaps not surprising that such a large discrepancy is seen in Fig. 2.

In support of the proposal that the collision frequency expression is in error for Si, we have performed the following crude analysis. The two-peak structure of  $g(r)$  for Si suggests, to a first approximation, that one can replace the quantity  $\sigma^2 g(\sigma)$  in Eq. (1) with the sum  $\sigma_1^2 g(\sigma_1) + \sigma_2^2 g(\sigma_2)$ , where the subscripts 1 and 2 refer to the positions of the two closely spaced peaks in  $g(r)$ . In other words we have effectively replaced the first nearest shell with two shells of atoms. It should be noted that the coordination number found by integrating  $g(r)$  over these first two peaks is 8. This simple two-shell model was applied to a representative Si data point and the new scaled  $D^*$  is indicated in Fig. 2 by the downward pointing arrow. The corrected data point is in quite good agreement with the EAM data. [The simple analysis could not be applied to every data point because at high temperatures the two peaks in  $g(r)$  merge to such an extent that the second position could not be defined. It is also interesting to note that at high temperatures where the  $g(r)$  approaches a single-peak structure the Si data approach those of the EAM.] Although the two-shell model is much too crude to draw quantitative conclusions, it does suggest that the source of the discrepancy for the case of Si stems from the approximate form used for the collision frequency and when the collision term is appropriately accounted for the resulting  $D^*$  scales with the entropy.

In summary, the simulation results presented here point to a number of caveats to the proposed scaling law of Dzugutov which relates the scaled liquid diffusivity to the excess entropy. For central force, multibody EAM potentials the scaling law is obeyed provided the actual excess entropy is used rather than the simple two-body  $S_2$  approximation. Also, the scaling law is valid for EAM binary mixtures, but a more general expression for the collision frequency is required. Finally, Dzugutov scaling does not hold for the case of Si as modeled by an interatomic poten-

tial which contains three-body angular dependent terms. It is proposed that the simple collision frequency term developed for hard spheres cannot adequately capture the more complicated local atomic structure observed in liquid Si.

This research was supported by the U.S. Department of Energy, Office of Basic Energy Sciences, Materials Science Division, under Contract No. DE-AC04-94AL85000.

- 
- [1] M. Dzugutov, *Nature (London)* **381**, 137 (1996).
  - [2] S. Chapman and T.G. Cowling, *The Mathematical Theory of Non-Uniform Gases* (Cambridge University Press, London, 1970).
  - [3] H.J. Raveche, *J. Chem. Phys.* **35**, 2242 (1971).
  - [4] F.H. Stillinger and T.A. Weber, *Phys. Rev. B* **31**, 5262 (1985).
  - [5] M.S. Daw and M.I. Baskes, *Phys. Rev. B* **29**, 6443 (1984).
  - [6] M.S. Daw, S.M. Foiles, and M.I. Baskes, *Mater. Sci. Rep.* **9**, 251 (1993); S.M. Foiles, in *Equilibrium Structure and Properties of Surfaces and Interfaces*, edited by A. Gonis and G.M. Stocks, NATO Advanced Study Institute, Ser. B, Vol. 300 (Plenum, New York, 1992).
  - [7] S.M. Foiles, *Phys. Rev. B* **32**, 3409 (1985).
  - [8] M. Asta, D. Morgan, J.J. Hoyt, B. Sadigh, J.D. Althoff, D. de Fontaine, and S.M. Foiles, *Phys. Rev. B* **59**, 14271 (1999).
  - [9] S.M. Foiles and J.B. Adams, *Phys. Rev. B* **40**, 5909 (1989).
  - [10] M.M.G. Alemany, C. Rey, and L.J. Gallego, *Phys. Rev. B* **58**, 685 (1998).
  - [11] M.M.G. Alemany, C. Rey, and L.J. Gallego, *J. Chem. Phys.* **109**, 5175 (1998).
  - [12] O. Rodriguez de la Fuente and J.M. Soler, *Phys. Rev. Lett.* **81**, 3159 (1998).
  - [13] J.J. Hoyt, B. Sadigh, M. Asta, and S.M. Foiles, *Acta Mater.* **47**, 3181 (1999).
  - [14] W. Yu, Z. Q. Wang, and D. Stroud, *Phys. Rev. B* **54**, 13946 (1996).
  - [15] S.M. Foiles, M.I. Baskes, and M.S. Daw, *Phys. Rev. B* **33**, 7983 (1986).
  - [16] A.F. Voter and S.P. Chen, *Mater. Res. Soc. Symp. Proc.* **82**, 175 (1987).
  - [17] J.P. Hansen and I.R. McDonald, *Theory of Simple Liquids* (Academic Press, London, 1976).
  - [18] Some of the scatter in Fig. 1 arises from the system sizes studied. For the 2048 cells used in the simulations the  $g(r)$  functions were truncated at about 14 Å and therefore it was necessary to check the convergence of the integral terms in Eq. (2). An estimate of the large  $r$  dependence showed that the truncation amounted to a lower value of  $S_2$  on the order of 2%–3%.
  - [19] A. Baranya and D.J. Evans, *Phys. Rev. A* **40**, 3817 (1989).
  - [20] J.G. Kirkwood, *J. Chem. Phys.* **3**, 300 (1935).
  - [21] J.-P. Hansen and L. Verlet, *Phys. Rev.* **184**, 151 (1969).
  - [22] J.K. Johnson, J.A. Zollweg, and K.E. Gubbins, *Mol. Phys.* **78**, 591 (1993).
  - [23] J.Q. Broughton and G.H. Gilmer, *J. Chem. Phys.* **79**, 5095 (1983).
  - [24] G. Jacucci and I.R. MacDonald, *Physica (Amsterdam)* **80A**, 607 (1975).